Analysis of Arbitrarily Oriented Microstrip Transmission Lines in Arbitrarily Shaped Dielectric Media over a Finite Ground Plane

JAYANTI VENKATARAMAN, MEMBER, IEEE, SADASIVA M. RAO, MEMBER, IEEE, ANTONIJE R. DJORDJEVIĆ, TAPAN K. SARKAR, SENIOR MEMBER, IEEE, AND YANG NAIHENG

Abstract—**A numerical analysis is presented for a multiconductor transmission line in multilayered lossy, dielectric regions where the ground plane is of finite extent. The transmission lines are infinitely long and vary in cross section from finite to infinitesimally thin. The Green's function for such a two-dimensional transmission line involves an arbitrary constant. If the ground plane is infinite, the method of images could be used where this constant cancels out. However, in the case of a finite ground plane, the constant has to be evaluated. Here a numerical method is presented where the constant could be eliminated rather than evaluated by imposing the condition for the total charge to be zero. The transmission lines, dielectric regions, and the ground plane can have arbitrary cross sections.**

I. Introduction

THE OBJECTIVE OF this analysis is to determine the capacitance and inductance matrix of a multiconductor transmission-line system. This work is an extension of the work described in [1]. The analysis is very general in the sense that both the conductors and the dielectric layers may be of arbitrary cross sections. The conductors are embedded in a multilayered dielectric material that is either above a single ground plane or contained between two ground planes. The ground planes may be of either infinite width or of finite width and may be arbitrarily oriented. Each dielectric-to-dielectric interface may also be of arbitrary shape and orientation while being homogenous along the axes of the transmission lines.

In spite of a large volume of literature available, there is no satisfactory analysis procedure to take care of such an arbitrary system of conductor and dielectric layer orientation. The present work has been developed to overcome this deficiency.

II. Analytical Formulation

The system under consideration is shown in Fig. 1(a), where a number of infinitely long, arbitrarily oriented striplines of arbitrary cross sections are embedded in several lossy homogenous dielectric layers. At first, the dielectrics are treated as lossless and then the losses are introduced by a complex dielectric permittivity. There are two important features of this system that should be noted. In order to have a more realistic and practical system, the dielectric layers are considered to be arbitrarily oriented, not necessarily parallel to one another or to the ground plane. Further, the ground plane is considered to be of finite extent. The numerical analysis is of course not limited to the finite ground plane. However, analysis by the method of images is carried out if the ground plane is infinite. The objective of this work is to develop a numerical method for analyzing arbitrarily oriented conductors embedded in dielectric layers with a finite ground plane.

In order to evaluate the capacitance, conductance, and inductance matrices of such a structure, the free charge on each of the conducting surfaces is required. The sum of the free charges and the polarization charges is related to the

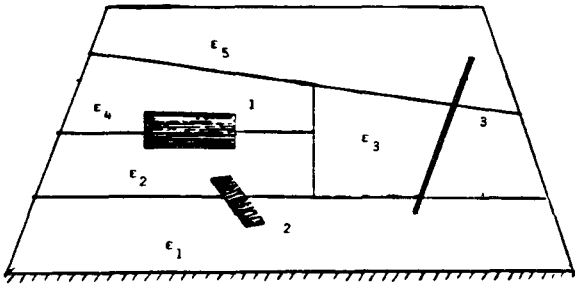

(a)

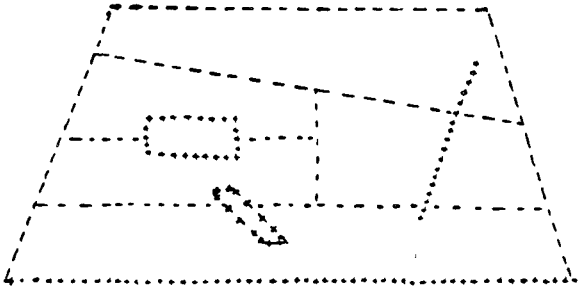

(b)

Fig. 1. (a) System configuration. (b) Equivalent system.

Manuscript received November 15, 1984; revised May 31, 1985. This work was supported in part by the Digital Equipment Corporation, Marlboro, MA.

J. Venkataraman and S. M. Rao are with the Department of Electrical Engineering, Rochester Institute of Technology, Rochester, NY 14623.

A. R. Djordjević is with the Department of Electrical Engineering, University of Belgrade, P.O. Box 816, Belgrade, Yugoslavia.

T. K. Sarkar is with the Department of Electrical Engineering, Syracuse University, Syracuse, NY 13210.

Yang Naiheng is with the Nanjing Research Institute of Electronic Technology, P.O. Box 315, Nanjing, Peoples Republic of China.

0018-9480/85/1000-0952$01.00 ©1985 IEEE

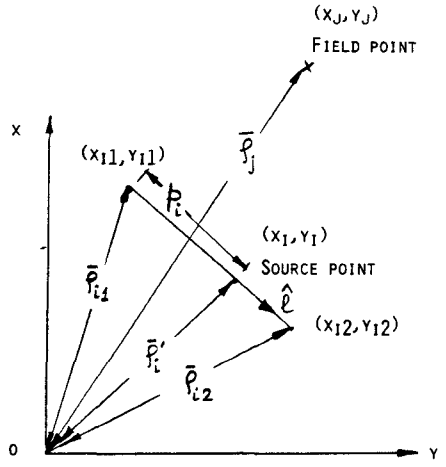

Fig. 2. Coordinate system of an arbitrarily oriented microstrip transmission line.

electric potentials and fields at the surface of any conductor and dielectric interface, respectively. With the help of the boundary conditions at the dielectric–dielectric and dielectric–conductor interfaces, the free charges can be obtained from the total charges.

The solution procedure is based on the well-known method of replacing all the conducting surfaces and dielectric layers by equivalent layers of unknown charge densities in free space as shown in Fig. 1(b). Under this condition, the potentials and electric field for the two-dimensional case are given by the familiar equations listed below:

$$V(\rho) = \frac{1}{2\pi\epsilon_0}\int_t \sigma_T(\rho')\ln\frac{K}{|\rho-\rho'|}\,dt \tag{1}$$

$$\boldsymbol{E} = -\nabla V(\rho) \tag{2}$$

where the integration is over the contour t of the strips and dielectric layers. V is the potential and $\boldsymbol{E}$ is the electric field. $\sigma_T(\rho')$ represents the total charge density which would be due to the sum of the bound and free charges at the conductor–dielectric boundaries and merely that due to the bound charges at the dielectric–dielectric interfaces, and K is an arbitrary constant to be determined.

With the coordinate systems described in Fig. 2, the electrostatic potential at any point ρ_j would be that due to the charge distribution at ρ_i'. If an infinite ground plane is present, the charge distribution due to its image is also included. All the conducting strips and dielectric–dielectric interfaces are divided into flat subsections and pulse functions are defined of the form

$$f_i(\rho) = \begin{cases} 1, & \text{on the } i\text{th subsection} \\ 0, & \text{elsewhere} \end{cases}. \tag{3}$$

The total charge density can now be expressed as follows:

$$\sigma_T \cong \sum \frac{q_i}{\Delta t_i} f_i(\rho) \tag{4}$$

where Δt_i is the contour of the ith subsection and q_i is the total charge on the ith conductor. The potential at each subsection on the conductor can be expressed in terms of the charges present everywhere. Hence, the potential at point (x_j, y_j) is

$$V_j = V(\rho_j) = \sum_{i=1}^{N} \frac{\sigma_{Ti}}{2\pi\epsilon_0}\int_{\Delta t_i} \ln\frac{K}{|\rho_j-\rho_i|}\,dt_i, \qquad j=1,2,\cdots,N_S. \tag{5}$$

Here

σ_{Ti} is the total charge density on the ith interface,
p_i is the contour of the ith subsection (as shown in Fig. 2),
$N = N_S + N_d$ is the total number of subsections,
N_S is the number of subsections on conductor surfaces,
N_d is the number of subsections on dielectric–dielectric interfaces.

Referring to Fig. 2, the distance $|\rho_j - \rho_i|$ between the source point and the field point can be expressed as follows:

$$|\rho_j-\rho_i| = \left\{|\rho_j-\rho_{i1}|^2 + p_i^2 - 2(\rho_j-\rho_{il})\cdot\hat{l}p_i\right\}^{1/2} \tag{6}$$

where $\hat{l}$ is the unit vector in the direction of the vector $(\rho_{i2}-\rho_{i1})$, where (x_{i2}, y_{i2}) and (x_{i1}, y_{i1}) denote the end coordinates of the ith subsection. With the help of a standard integral, (5) reduces to the following form:

$$V_j = \sum_{i=1}^{N}\left[\frac{\sigma_{Ti}}{2\pi\epsilon_0}\Delta t_i \ln K + \frac{\sigma_{Ti}}{2\pi\epsilon_0}(R_{j2}-R_{j1}) + R_{12} - R\tan^{-1}\left(\frac{RR_{12}}{S}\right)\right] \tag{7}$$

where

$$\begin{aligned} R_{j1} &= \left[(\rho_j-\rho_{i1})\cdot\hat{l}\right]\ln|\rho_j-\rho_{i1}| \\ R_{j2} &= \left[(\rho_j-\rho_{i2})\cdot\hat{l}\right]\ln|\rho_j-\rho_{i2}| \\ R_{12} &= |\rho_2-\rho_{i1}| \\ R &= \left\{|\rho_j-\rho_{i1}|^2 - \left[(\rho_j-\rho_{i1})\cdot\hat{l}\right]^2\right\}^{1/2} \\ S &= (\rho_j-\rho_{i1})\cdot(\rho_j-\rho_{i2}). \end{aligned} \tag{8}$$

Δt_i is the length of the ith subsection. In the above equations, the coordinate locations of the ith and jth interfaces or subsections are used so that angles of orientation do not have to be specified in the $x-y$ plane. Hence

$$(\rho_j-\rho_{i1}) = \hat{a}_x(x_j-x_{i1}) + \hat{a}_y(y_j-y_{i1}) \tag{9}$$

$$(\rho_j-\rho_{i2}) = \hat{a}_x(x_j-x_{i2}) + \hat{a}_y(y_j-y_{i2}) \tag{10}$$

$$(\rho_{i2}-\rho_{i1}) = \hat{a}_x(x_{i2}-x_{i1}) + \hat{a}_y(y_{i2}-y_{i1}) \tag{11}$$

$$\hat{l} = \frac{(\rho_{i2}-\rho_{i1})}{|\rho_{i2}-\rho_{i1}|}. \tag{12}$$

Simplifying (8) by using (9)–(12), we obtain the necessary equations for any arbitrary orientation of conductors, dielectric layers, and ground plane. The total $N = N_S + N_d$ equations are used to solve for the unknowns σ_{Ti}, $i = 1,2,\cdots,N$. We utilize the continuity of the potential for the first N_S equations on a conductor surface and equate the continuity of the normal components of the fields in the remainder of the N_d equations.

The boundary conditions at any dielectric–dielectric interface yield the following:

$$\left.\begin{aligned} \boldsymbol{D}_1\cdot\hat{n} &= \boldsymbol{D}_2\cdot\hat{n} \\ \boldsymbol{E}_2\cdot\hat{n} &= \frac{\epsilon_1}{\epsilon_2}\boldsymbol{E}_1\cdot\hat{n} \end{aligned}\right\} \tag{13}$$

where the outward normal $\hat{n}$ is defined in Fig. 3 and ϵ_1 and ϵ_2 are the dielectric permittivities of the two regions. Also, at the same boundary, the bound charge density σ_b can be expressed in terms of the polarization vectors $\boldsymbol{P}_1$ and $\boldsymbol{P}_2$

$$\sigma_b = (\boldsymbol{P}_1 - \boldsymbol{P}_2)\cdot\hat{n}. \tag{14}$$

Using (13), (14) reduces to

$$\sigma_b = \left(\frac{\epsilon_{r1}-\epsilon_{r2}}{\epsilon_{r1}}\right)\epsilon_0 \boldsymbol{E}_2\cdot\hat{n} \tag{15}$$

where ϵ_{r1} and ϵ_{r2} are the relative permittivities of the two regions.

The electric field $\boldsymbol{E}_j$ at any subsection located at a dielectric interface due to charge distributions at all the interfaces can be expressed as follows:

$$\boldsymbol{E}_j\cdot\hat{n} = \boldsymbol{E}(\rho_j)\cdot\hat{n} = \sum_{\substack{i=1\\ i\neq j}}^{N} \frac{\sigma_{Ti}}{2\pi\epsilon_0}\int_{t_i}\frac{(\rho_j-\rho_i)}{|\rho_j-\rho_i|}\cdot\hat{n}\,dt_i + \frac{\sigma_{Tj}}{2\epsilon_0}. \tag{16}$$

When the interfaces are flat, the integral reduces to

$$\begin{aligned} I &= \int_{t_i}\frac{(\rho_j-\rho_i)}{|\rho_j-\rho_i|^2}\cdot\hat{n}\,dt_i \\ &= \frac{1}{2}(L1)\ln\left(\frac{R1^2}{R}\right) + L1\cdot RL - RN\cdot F1 \end{aligned} \tag{17}$$

where

$$F1 = \begin{cases} \dfrac{1}{RL} + \dfrac{1}{(R12-RL)}, & \Delta = 0 \\ \dfrac{1}{\sqrt{\Delta}}\left[\tan^{-1}\left(\dfrac{RL}{\sqrt{\Delta}}\right) - \tan^{-1}\left(\dfrac{R12-RL}{\sqrt{\Delta}}\right)\right], & \Delta > 0 \end{cases}$$

$$\Delta = |\rho_j-\rho_{i1}|^2 - [(\rho_j-\rho_{i1})\cdot\hat{l}]^2$$
$$R1 = |\rho_j-\rho_{i1}|$$
$$R12 = |\rho_{i2}-\rho_{i1}|$$
$$RN = (\rho_j-\rho_{i1})\cdot\hat{n}$$
$$RL = (\rho_j-\rho_{i1})\cdot\hat{l}$$
$$L1 = \hat{l}\cdot\hat{n}$$
$$R = |\rho_j-\rho_{i1}|^2 + |\rho_{i2}-\rho_{i1}|^2 - 2(\rho_j-\rho_{i1})\cdot\hat{l}\,|\rho_{i2}-\rho_{i1}|.$$

From (15) and (16), one obtains the following equation:

$$\sigma_{Tj}\frac{(\epsilon_{ir1}+\epsilon_{ir2})}{\epsilon_0} - (\epsilon_{ir1}-\epsilon_{ir2})\sum_{\substack{i=1\\ i\neq j}}^{N}\frac{\sigma_{Ti}}{2\pi\epsilon_0}\int_{t_i}\frac{(\rho_j-\rho_i)}{|\rho_j-\rho_i|^2}\cdot\hat{n}\,dt_i = 0. \tag{18}$$

The moment method formulation reduces N_s equations of the form (7) and N_d equations of the form (18) to a matrix equation, denoted by

$$\begin{bmatrix} Z_{11} & \cdots & Z_{1N} \\ Z_{21} & & Z_{2N} \\ \vdots & & \vdots \\ Z_{N1} & \cdots & Z_{NN} \end{bmatrix}\begin{bmatrix} \sigma_1 \\ \sigma_2 \\ \vdots \\ \sigma_N \end{bmatrix} = \begin{bmatrix} V_1 \\ V_2 \\ \vdots \\ V_{N_s} \\ 0 \\ 0 \end{bmatrix}$$

that is

$$[Z][\sigma] = [V]. \tag{19}$$

In order to calculate the electrical parameters, the free-charge densities at the various conductors should be obtained. If the ground plane is infinite, the constant K in (7) is eliminated because of the image term, and the free charges may be obtained as described later in Section III. However, for a finite ground plane or when the conductors have different voltages, then this constant has to be evaluated. Instead of evaluating this constant, a numerical scheme has been devised to eliminate it.

The method essentially forces the total of the bound and free charges on all conducting surfaces and dielectric layers to be equal to zero. Numerically, it would amount to subtracting the elements of the first row of the $[Z]$ matrix from the corresponding elements of all the other rows from $i=2$ to $i=N_s$ and then replacing the first row by the lengths of the corresponding subsections. As for the $[V]$ vector, the first element is subtracted from all other elements including the first one. Therefore, (19) would become

$$\begin{bmatrix} l_1 & l_2 & l_3 & \cdots & l_N \\ (Z_{21}-Z_{11}) & (Z_{22}-Z_{12}) & (Z_{23}-Z_{13}) & \cdots & (Z_{2N}-Z_{1N}) \\ \vdots & & & & \vdots \\ (Z_{N_s,1}-Z_{11}) & (Z_{N_s,2}-Z_{12}) & (Z_{N_s,3}-Z_{13}) & & (Z_{N_s,N}-N_{1N}) \\ Z_{N_{s+1},1} & Z_{N_s+1,2} & Z_{N_{s+1},3} & & Z_{N_{s+1},N} \\ \vdots & & & & \vdots \\ Z_{N,1} & Z_{N,2} & \cdot & & Z_{N,N} \end{bmatrix}\begin{bmatrix} \sigma_1 \\ \sigma_2 \\ \vdots \\ \sigma_{N_s} \\ \vdots \\ \sigma_N \end{bmatrix} = \begin{bmatrix} 0 \\ V_2-V_1 \\ V_3-V_1 \\ \vdots \\ V_{N_s}-V_1 \\ 0 \\ \vdots \\ 0 \end{bmatrix}. \tag{20}$$

III. Evaluation of the Free-Charge Density

The analysis here treats a system of both finite thickness and zero thickness conductors. A commonly used procedure for treating finite dimension conductors would be to use the boundary conditions at its boundaries, which would require the normal component of the electric flux density

Fig. 3. Boundary conditions for electric fields.

vector to be equal to the free-charge density since the field within the conductor is equal to zero. However, a problem is encountered when the conductors are of unequal dimensions. When they are of the same thickness, the mutual capacitance C_{12} and C_{21}, etc., are exactly equal [1]. But in a system of transmission lines of unequal thicknesses, this is no longer true and the difference becomes most pronounced when some of the conductors are of finite thickness and some are infinitely thin. This could be because the numerical method of modeling using point matching may not give a zero field inside the conductor, a condition used in developing the boundary conditions at the surface of a conductor.

To overcome this difficulty, the present analysis considers all conducting surfaces as interfaces which for infinitely thin conductors would have the two dielectric regions on either side, and for finite-dimensioned conductors would have a dielectric region on one side and the dielectric permittivity ϵ_0 corresponding to a conductor on the other.

With an arbitrary orientation of the various interfaces and the outward normal as defined in Fig. 3, the free-charge density σ_{fj} at the jth subsection is as follows:

$$\sigma_{fj} = (\boldsymbol{D}_2 - \boldsymbol{D}_1)\cdot\hat{n}_j \tag{21}$$

which is equivalent to

$$\sigma_{fj} = (\epsilon_{r1} - \epsilon_{r2})\epsilon_0 \boldsymbol{E}_2\cdot\hat{n}_j + \epsilon_{r1}\sigma_{Tj} \tag{22}$$

where σ_{Tj} is the total charge density.

Using (16), (22) reduces to the following:

$$\sigma_{fj} = \frac{(\epsilon_{r1}+\epsilon_{r2})}{2}\sigma_{Tj} + \frac{(\epsilon_{r2}-\epsilon_{r1})}{2\pi}\sum_{\substack{i=1\\ i\neq j}}^{N}\sigma_{Ti}\int_{ti}\frac{(\rho_i - \rho')}{|\rho_j - \rho'|^2}\cdot\hat{n}\,dt_i. \tag{23}$$

Equation (23) can be expressed conveniently in a matrix form

$$\begin{bmatrix} Z'_{11} & Z'_{12} & \cdots & Z'_{1N} \\ \vdots & & & \\ Z'_{N_s,2} & Z'_{N_s,1} & \cdots & Z'_{N_s,N} \end{bmatrix}\begin{bmatrix}\sigma_1 \\ \vdots \\ \sigma_N\end{bmatrix} = \begin{bmatrix}\sigma_{f1} \\ \sigma_{f,N_s}\end{bmatrix} \tag{24}$$

$$[Z'][\sigma_T] = [\sigma_f] \tag{25}$$

where

$\sigma_{fi}, i = 1,2,\cdots, N_s$ is the free-charge density at the conductor–dielectric interfaces.

Once the free-charge density is obtained from (19), then from (25) the total free charges q_i on the ith subsection can be evaluated from the following equation:

$$q_{fi} = \sigma_{fi}\Delta t_i \tag{26}$$

where Δt_i is the length of the ith subsection.

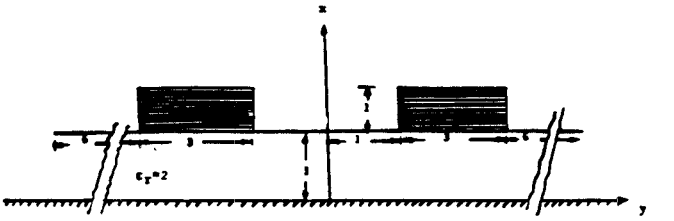

Fig. 4. Microstrip transmission-line system where the conducting strips are of finite thickness. Solution is by the method of images.

IV. Capacitance and Inductance Matrix

Any element of the electrostatic induction matrix C_{ij} may be defined as the ratio of the total charge on the ith conductor to the potential on the jth conductor with all other conductors at zero potential. Hence

$$C_{ij} = \left.\frac{q_i}{V_j}\right|_{\substack{V_k=0,\\ k\neq j.}}^{k=1,2,\cdots} \tag{27}$$

In order to obtain the inductance matrix, capacitance matrix C_0 is calculated for the striplines oriented exactly as before except that they exist in free space and are not embedded in the dielectric layers. The inductance per unit length is related to the capacitance per unit length by the following relation [1]:

$$[L] = \frac{1}{c^2}[C_0]^{-1} \tag{28}$$

where c is the speed of light in free space.

V. Dielectric Losses and the Conductance Matrix

The microstrip transmission-line system discussed above is now considered with multilayered, arbitrarily oriented lossy dielectrics associated with a complex dielectric permittivity $\hat{\epsilon}$. There is an additional transmission-line parameter, namely, the conductance matrix $[G]$, which is the analog of the capacitance matrix.

The coupled complex time-harmonic transmission-line equations for the voltage and current are of the form given below:

$$\frac{d\hat{V}}{dz} = -j\omega[L]\hat{I} \tag{29}$$

$$\frac{d\hat{I}}{dz} = -\{[G] + j\omega[C]\}\hat{V} = [\hat{Y}]\hat{V} \tag{30}$$

where the complex permittivity $\hat{\epsilon}$, which gives rise to the admittance matrix $[\hat{Y}]$, is expressed as

$$\hat{\epsilon} = \epsilon' - j\epsilon'' \text{ with the loss tangent } \tan\delta = \frac{\epsilon''}{\epsilon'}.$$

A time variation of the $e^{j\omega t}$ has been assumed. Equation (30) can be written as follows:

$$\frac{d\hat{I}}{dz} = -j\omega\left\{[C] + \frac{[G]}{j\omega}\right\}\hat{V} = -j\omega[\hat{C}]\hat{V} \tag{31}$$

TABLE I
RESULTS FOR THE MICROSTRIP TRANSMISSION-LINE SYSTEM SHOWN IN FIG. 4

	Present Analysis	Weeks [2]	Rao and Sarkar [3]
$C_{11} = C_{22}$ pF/m	92.36	92.24	91.89
$C_{12} = C_{21}$ pF/m	-8.494	-8.504	-7.019
$L_{11} = L_{22}$ μH/m	0.1982	0.1982	0.1855
$L_{12} = L_{21}$ μH/m	0.03014	0.02980	0.02361

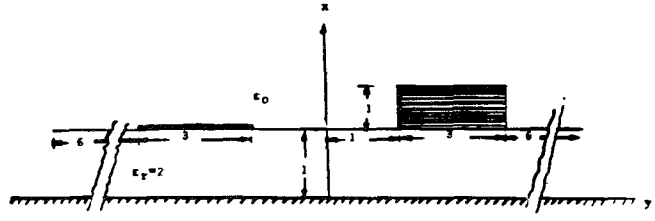

Fig. 5. Microstrip transmission-line system where one conductor is of finite thickness and the other is of zero thickness. Solution is by the method of images.

where the complex matrix

$$[\hat{C}] = [C] + \frac{[G]}{j\omega}. \tag{32}$$

Using the same solution procedure as described in the previous sections but with complex dielectric permittivities, one could obtain the complex matrix $[\hat{C}]$. Using (32), this matrix can be related to the capacitance and conductance matrices by the capacitance matrix

$$[C] = \mathrm{Re}[\hat{C}] \tag{33}$$

and the conductance matrix

$$[G] = -\omega\,\mathrm{Im}[\hat{C}] \tag{34}$$

ω being the angular frequency.

All the merits of this analysis already discussed still hold for this complex case. The system is very general with arbitrary oriented conductors and dielectric layers of arbitrary cross section. Ground planes could be present and they could be finite or infinite in size. The system of conductors and dielectrics could also be sandwiched between two finite ground planes. Further, a condition has been imposed to make the total charge, the sum of the free charges and polarization charges, equal to zero. The conductor–dielectric interfaces are treated in the same way as dielectric–dielectric interfaces with ϵ_0 used for the permittivity of the conductor. This is to make sure that the total field within the conductor is equal to zero, a condition not necessarily true when using point matching for the solution procedure. It is seen here that this last condition and the one for the total charge to be zero results in a very nearly symmetric capacitance and conductance matrices when the conductors are of unequal cross section.

VI. RESULTS

To illustrate the numerical analysis developed here, the commonly used microstrip transmission lines with two conductors mounted above a ground plane have been considered. The microstrip transmission-line system and results for the capacitance and inductance matrices are presented for each of the following examples. As a first example, consider the configuration given in Fig. 4. The results for that configuration (Table I) are compared with those obtained by Weeks [2] for the two-dimensional case by Rao and Sarkar [3] for the three-dimensional case. The agreement is satisfactory.

For the same configuration, the various features of this analysis have been demonstrated. To illustrate its use for conductors of various thicknesses, one of the conductors was reduced to zero thickness (Fig. 5). The results in Table II show a difference of less that 0.1 percent in the values of C_{12} and C_{21}. Table III for the system in Fig. 6 shows the case when both conductors have been reduced to zero thickness. Table IV illustrates the effects of the dielectric edges for the system in Fig. 7. Comparison of this table with Table I shows that there is a relatively small change in the capacitance as the width of the dielectric is reduced. Next, the ground plane has been treated as a finite conductor with zero voltage, as shown in Fig. 8. The results of Table V compare well with those of a similar configuration (Table IV) where the ground plane is infinite. Table VI, corresponding to Fig. 9, illustrates the same kind of analysis as Table V, except that one of the conductors is of zero thickness.

The total number of subsections in each example is about 150. For example, in Table V for Fig. 8, where the ground plane is finite and the dielectric edges have been taken into account, the subsections used were as follows: there were 12 subsections on the ground plane, 8 subsections each along the Y-direction of each conductor, 2 subsections each along the X-direction of each conductor, 8 subsections each along the vertical dielectric edges and along the horizontal dielectric–air interface, 10 subsections from the edge of the dielectric to the conductor, 8 subsections between the conductors, and 10 subsections again from the edge of the conductor to the dielectric.

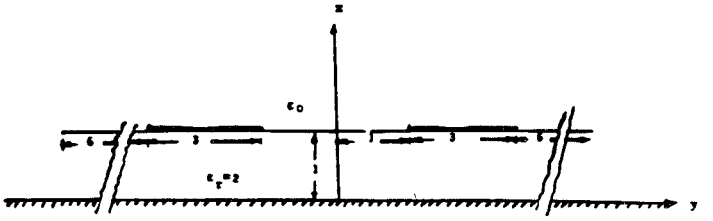

Fig. 6. Microstrip transmission-line system where the conducting strips are of zero thickness. Solution is by the method of images.

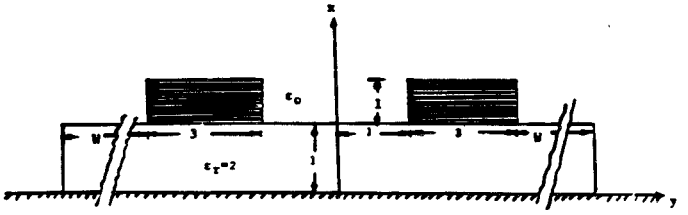

Fig. 7. Microstrip transmission-line system with W varying. The effect of the dielectric edges has been illustrated for two cases when the edges are included and when they are excluded.

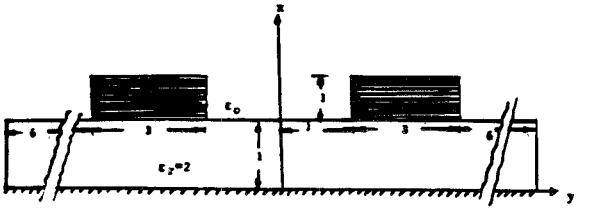

Fig. 8. Microstrip transmission-line system of finite thickness conducting strips. The edges of the dielectric have been taken into account. The ground plane has been treated as a conducting strip.

TABLE II
RESULTS FOR THE MICROSTRIP TRANSMISSION-LINE SYSTEM SHOWN IN FIG. 5

Capacitance Matrix	Inductance Matrix
C_{11} = 91.24 (pF/m)	L_{11} = 0.2006 (μH/m)
C_{22} = 83.16 (pF/m)	L_{22} = 0.2317 (μH/m)
C_{12} = -5.602 (pF/m)	L_{12} = 0.023704 (μH/m)
C_{21} = -5.647 (pF/m)	L_{21} = 0.023703 (μH/m)

TABLE III
RESULTS FOR THE MICROSTRIP TRANSMISSION-LINE SYSTEM SHOWN IN FIG. 6

Capacitance Matrix	Inductance Matrix
C_{11} = 82.514 (pF/m)	L_{11} = 0.2335 (μH/m)
C_{22} = 82.594 (pF/m)	L_{22} = 0.2335 (μH/m)
C_{12} = -3.827 (pF/m)	L_{12} = 0.01885 (μH/m)
C_{21} = -3.827 (pF/m)	L_{21} = 0.01885 (μH/m)

TABLE IV
RESULTS FOR THE MICROSTRIP TRANSMISSION-LINE SYSTEM SHOWN IN FIG. 7

W	$C_{11} = C_{22}$ (pF/m)		$C_{12} = C_{21}$ (pF/m)	
	Without Edge	With Edge	Without Edge	With Edge
6.0	92.36	92.05	-8.494	-8.473
4.0	92.44	92.14	-8.506	-8.485
2.0	92.40	92.10	-8.539	-8.517
0.5	91.44	90.50	-8.595	-8.565
0.0	89.68	87.97	-8.603	-8.569

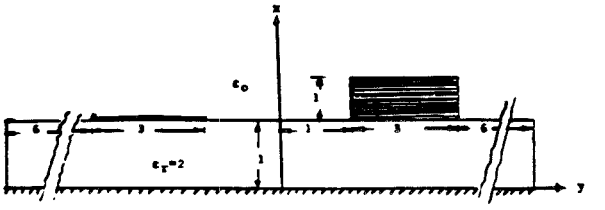

Fig. 9. Microstrip transmission-line system where one conductor is of finite thickness and the other is of zero thickness. The ground plane is treated as a finite conductor. The edges of the dielectric have been taken into account.

TABLE V
RESULTS FOR THE MICROSTRIP TRANSMISSION-LINE SYSTEM SHOWN IN FIG. 8

Capacitance Matrix	Inductance Matrix
$C_{11} = C_{22}$ = 91.642 (pF/m)	$L_{11} = L_{22}$ = 0.20035 (μH/m)
$C_{12} = C_{21}$ = -8.6972 (pF/m)	$L_{12} = L_{21}$ = 0.031826 (μH/m)

TABLE VI
RESULTS FOR THE MICROSTRIP TRANSMISSION-LINE SYSTEM SHOWN IN FIG. 9

Capacitance Matrix	Inductance Matrix
C_{11} = 90.43 (pF/m)	L_{11} = 0.2028 (μH/m)
C_{22} = 82.703 (pF/m)	L_{22} = 0.2336 (μH/m)
C_{12} = -5.73295 (pF/m)	L_{12} = 0.025023 (μH/m)
C_{21} = -5.79379 (pF/m)	L_{21} = 0.025020 (μH/m)

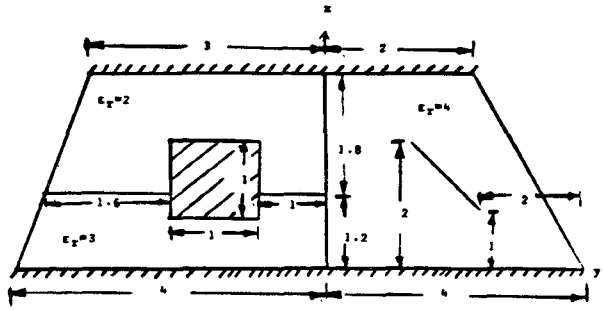

Fig. 10. Microstrip transmission-line system with two ground planes of finite dimension and two conductors of which one is infinitely thin. The dielectric layers are oriented as shown.

TABLE VII
RESULTS FOR THE MICROSTRIP TRANSMISSION-LINE

Capacitance Matrix		Inductance Matrix	
C_{11} = 114.9	(pF/m)	L_{11} = 0.2368	(μH/m)
C_{22} = 104.7	(pF/m)	L_{22} = 0.3745	(μH/m)
C_{12} = -7.097	(pF/m)	L_{12} = 0.01986	(μH/m)
C_{21} = -7.21	(pF/m)	L_{21} = 0.01986	(μH/m)

TABLE VIII
RESULTS FOR THE SYSTEM SHOWN IN FIG. 11

	Present Analysis	Harrington [4]	Analytical
C (pF/m)	80.093	80.08	80.37
G (S/m)	0.6032×10^{-4}	0.6038×10^{-4}	0.606×10^{-4}
L (μH/m)	0.5530	0.555	0.5537

TABLE IX
RESULTS FOR THE MICROSTRIP TRANSMISSION-LINE SYSTEM SHOWN IN FIG. 12

I	J	Capacitance Matrix (pF/m)		Inductance Matrix (μH/m)		Conductance Matrix (μS/m)	
		Present Analysis	Harrington [4]	Present Analysis	Harrington [4]	Present Analysis	Harrington [4]
1	1	301.21	308.8	0.26786	0.2714	0.6294	0.6420
1	2	-36.82	-36.06	0.04441	0.0449	-0.17182	-0 1701
1	3	-2.636	-2.848	0.01273	0.01295	-0.01257	-0.01327
1	4	-22.28	-24.59	0.03317	0.03442	-0.05818	-0.0607
2	1	-36.98	-36.06	0.4456	0.04488	-0.1736	-0.1701
2	2	343.41	333.1	0.2520	0.2594	1.5119	1.481
2	3	-27.17	-30.45	0.03339	0.03447	-0.1384	-0.1498
2	4	-17.23	-16.41	0.03692	0.03742	-0.09854	-0.09688
3	1	-2.712	-2.848	0.01284	0.01295	-0.01242	-0.01327
3	2	-27.08	-30.45	0.03335	0.03447	-0.13511	-0.1498
3	3	358.99	380.6	0.25592	0.2570	1.5296	1.608
3	4	-32.26	-31.78	0.052788	0.0525	-0.1776	-0.1777
4	1	-24.37	-24.59	0.033983	0.03447	-0.05944	-0.0607
4	2	-16.73	-16.41	0.03699	0.03742	-0.09941	-0.09688
4	3	-31.32	-31.78	0.052687	0.0525	-0.1760	-0.1777
4	4	230.5	232.8	0.32655	0.3326	0 6341	0 6383

As a final example, we consider a finite-thickness conductor and a zero-thickness arbitrarily oriented conducting strip sandwiched between two finite-length ground planes containing various dielectric layers as illustrated in Fig. 10. The capacitance and the inductance matrices for this configuration are given in Table VII. In this case, the discrepancy between C_{12} and C_{21} is less that 2 percent.

The examples given above illustrate the microstrip transmission line with arbitrarily oriented dielectric layers and a finite ground plane.

When the dielectrics are lossy, the conductance matrix can be evaluated for a similar microstrip transmission-line system described above. Tables VIII and IX, corresponding to Figs. 11 and 12, respectively, are two examples which have been compared to the results of Harrington *et al.* [4]. It should be noted that the difference in the elements $C_{n,m}$ and $C_{m,n}$ shown in Table IX ranges between 0.3 to about 8 percent. These values have not been averaged as in [4].

VII. CONCLUSION

A numerical procedure has been presented for the computation of inductance, capacitance, and conductance matrices for arbitrarily oriented multiconductor transmis-

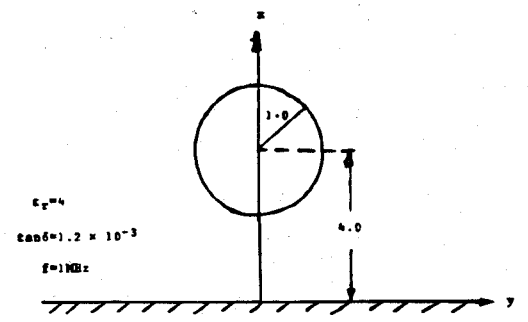

Fig. 11. A circular conductor above a perfectly conducting, infinite ground plane. Solution is by the method of images.

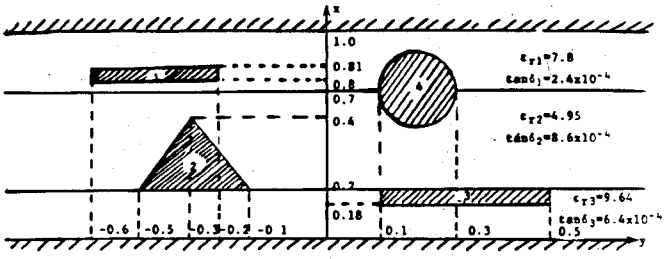

Fig. 12. Microstrip transmission-line system of four conducting lines embedded in three lossy dielectric layers and placed between two ground planes.

sion lines of arbitrary cross sections in multiple dielectric media. The conductors may be of finite cross section or may be strips of zero thickness. The dielectric layers can be of arbitrary orientation. The conductors embedded in the multilayered dielectrics can be either on top of a finite or infinitely wide ground plane or sandwiched between two arbitrarily oriented ground planes.

References

[1] C. Wei, R. F. Harrington, J. R. Mautz, and T. K. Sarkar, "Multiconductor transmission lines in multilayered dielectric media," *IEEE Trans. Microwave Theory Tech.*, vol. MTT-32, pp. 439–450, Apr. 1984.

[2] W. T. Weeks, "Calculation of coefficients of capacitance of multiconductor transmission lines in the presence of dielectric interface," *IEEE Trans. Microwave Theory Tech.*, vol. MTT-18, pp. 35–43, Jan. 1980.

[3] S. M. Rao, T. K. Sarkar, and R. F. Harrington, "The electrostatic field of conducting bodies in multiple dielectric media," *IEEE Trans. Microwave Theory Tech.*, vol. MTT-32, pp. 1441–1448, Nov. 1984.

[4] R. F. Harrington and C. Wei, "Lossess on multiconductor transmission lines in multilayered dielectric media," *IEEE Trans. Microwave Theory Tech.*, vol. MTT-32, pp. 705–710, July 1984.

Jayanti Venkataraman (M'81) was born in Bangalore, India. She received the B.S. and M.S. degrees in 1969 and 1971, respectively, from the Bangalore University, Bangalore, India. In 1977, she received the Ph.D. degree in electrical engineering from the Indian Institute of Science, Bangalore, India, and continued as Research Associate at the same place until 1980.

Since 1982, she has been an Assistant Professor in the Electrical Engineering Department, Rochester Institute of Technology, Rochester, New York. Between 1980–1981, she was a Research Associate at the Physical Science Laboratory, Las Cruces, New Mexico. From 1981–1982, she was a Research Associate at the Electromagnetics Laboratory, University of Colorado, Boulder, CO. Her interests are in the area of integrated microwave and millimeter-wave antennas and circuits.

Antonije R. Djordjević was born in Belgrade, Yugoslavia, in 1952. He received the B.Sc., M.Sc., and D.Sc. degrees from the University of Belgrade in 1975, 1977, and 1979, respectively.

In 1975, he joined the Department of Electrical Engineering, University of Belgrade, as a Teaching Assistant in Electromagnetics. In 1982, he was appointed as Assistant Professor in Microwaves at the same department. From February 1983 until February 1984, he was with the Department of Electrical Engineering, Rochester Institute of Technology, Rochester, NY, as a Visiting Associate Professor. His research interests are numerical problems in electromagnetics, especially those applied to antennas and microwave passive components.

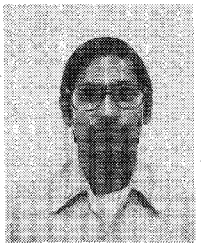

Sadasiva M. Rao (M'83) received the Bachelors degree in electrical and communication engineering from Osmania University, Hyderabad, India, in 1974, the Masters degree in 1976 from the Indian Institute of Sciences, Bangalore, India, and the Ph.D. degree from the University of Mississippi, University, MS, in 1980.

Since 1976, he has been a Research Assistant in the Department of Electrical Engineering at the University of Mississippi. Currently, he is an Assistant Professor at Rochester Institute of Technology, Rochester, NY. His research interests are in the areas of electromagnetic theory and numerical methods applied to antennas and scattering.

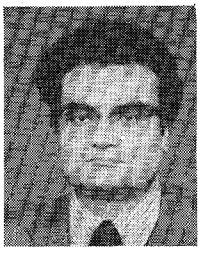

Tapan K. Sarkar (S'69–M'76–SM'81) was born in Calcutta, India, on August 2, 1948. He received the B.Tech. degree from the Indian Institute of Technology, Kharagpur, India, in 1969, the M.Sc.E. degree from the University of New Brunswick, Fredericton, NB, Canada, in 1971, and the M.S. and Ph.D. degrees from Syracuse University, Syracuse, NY, in 1975.

From 1969 to 1971, he served as an Instructor at the University of New Brunswick. While studying at Syracuse University, he served as an Instructor and Research Assistant in the Department of Electrical Engineering. From 1976 to 1985, he was with Rochester Institute of Technology, Rochester, NY. From 1977 to 1978, he was a Research Fellow at the Gordon McKay Laboratory of Harvard University, Cambridge, MA. Presently, he is with the Department of Electrical and Computer Engineering at Syracuse University, Syracuse, NY. His current research interests deal with numerical solution of operator equations arising in electromagnetics and signal processing with application to system identification.

Dr. Sarkar is a Registered Professional Engineer in the state of New York. He is a member of Sigma Xi and International Union of Radio Science Commissions A and B.

Yang Naiheng was born in Zhejiang, China, in 1942. He graduated from the Department of Electromagnetic Physics, Chinese University of Science and Technology, Beijing, China, in 1965.

Since then he has worked at Nanjing Research Institute of Electronics and Technology, Nanjing, China. He has done research work in the areas of microwave feed systems and components, such as digital phase shifters, switches, and directional couplers. In November 1980, he came to Syracuse University, Syracuse, NY, as a Visiting Scholar.